SCIENTIFIC REPORTS

OPEN

Pressure-induced superconductivity in H_2-containing hydride $PbH_4(H_2)_2$

Ya Cheng[1], Chao Zhang[2], Tingting Wang[1], Guohua Zhong[1], Chunlei Yang[1], Xiao-Jia Chen[3] & Hai-Qing Lin[1,4]

High pressure structure, stability, metallization, and superconductivity of $PbH_4(H_2)_2$, a H_2-containing compound combining one of the heaviest elements with the lightest element, are investigated by the first-principles calculations. The metallic character is found over the whole studied pressure range, although $PbH_4(H_2)_2$ is metastable and easily decompose at low pressure. The decomposition pressure point of 133 GPa is predicted above which $PbH_4(H_2)_2$ is stable both thermodynamically and dynamically with the $C2/m$ symmetry. Interestedly, all hydrogen atoms pairwise couple into H_2 quasi-molecules and remain this style up to 400 GPa in the $C2/m$ structure. At high-pressure, $PbH_4(H_2)_2$ tends to form the Pb-H_2 alloy. The superconductivity of T_c firstly rising and then falling is observed in the $C2/m$ $PbH_4(H_2)_2$. The maximum of T_c is about 107 K at 230 GPa. The softening of intermediate-frequency phonon induced by more inserted H_2 molecules is the main origin of the high T_c. The results obtained represent a significant step toward the understanding of the high pressure behavior of metallic hydrogen and hydrogen-rich materials, which is helpful for obtaining the higher T_c.

In recent decades, many scientists have devote to searching for the high-temperature superconducting materials. For the lightest element, hydrogen (H), Ashcroft applied the BCS theory to propose that the metallic hydrogen will be a room-temperature superconductor under high pressure[1]. This suggestion has motivated considerable experimental and theoretical activities. However, solid hydrogen remains insulating character at extremely high pressure, at least up to 342 GPa[2]. Due to the extremely high and experiment unreachable pressure, as a alternative, Ashcroft proposed that the hydrogen-rich alloys shall transform into metal under relatively lower pressure due to the chemical precompressions from the comparable weight elements[3]. Thus, hydrogen-rich group-IV hydrides have been extensively explored, such as CH_4, SiH_4, GeH_4, SnH_4, and PbH_4. All of them show up interesting new structures and novel properties under pressure. CH_4 is still an insulator up to the pressure of 520 GPa[4]. Although Eremets *et al.* experimentally reported the metallization and superconductivity of SiH_4 above 60 GPa[5], for the controversial result it might be understood as superconductivity of amorphous silicon, silicon hydrides, or platinum hydrides[6,7]. And theoretical prediction indicates that the stable SiH_4 can behave as metal and exhibit superconductivity above 220 GPa with the superconducting transition temperature (T_c) of about 20 K (The Coulomb parameter $\mu^* = 0.1$, the below is same.)[8]. GeH_4 has lower metallization pressure than silane[9,10], and the highest T_c reaches to 73 K at 220 GPa[11]. Furthermore, the metallization pressure of SnH_4 decreases, the highest T_c is close to 83 K at 120 GPa[12].

It is clearly that the metallization pressure of group-IV hydrides decreases with increase of atomic number of heavy element, which is obviously less than that of solid H_2. Unfortunately, the T_c of group-IV hydrides is also greatly decreased. By analyzing the crystal feature, we find that the quasi-molecular H_2

[1]Shenzhen Institutes of Advanced Technology, Chinese Academy of Sciences and The Chinese University of Hong Kong, Shenzhen, 518055, China. [2]Department of Physics, Yantai University, Yantai, 264005, China. [3]Center for High Pressure Science and Technology Advanced Research, Shanghai 201203, China. [4]Beijing Computational Science Research Center, Beijing 100089, China. Correspondence and requests for materials should be addressed to G.Z. (email: gh.zhong@siat.ac.cn) or C.Y. (email: cl.yang@siat.ac.cn)
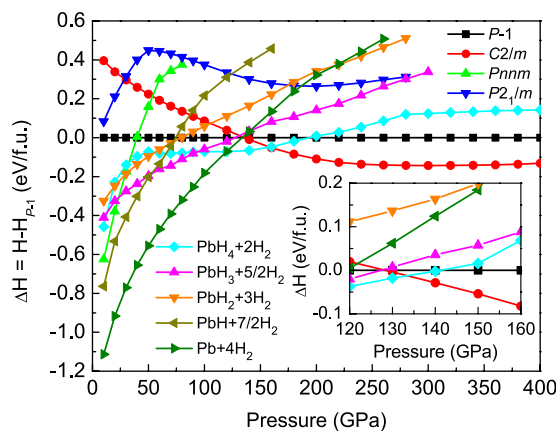
Figure 1. Calculated enthalpies per PbH$_4$(H$_2$)$_2$ unit as the function of pressure. Enthalpy difference versus pressure for competitive structures of PbH$_4$(H$_2$)$_2$, referenced to the P-1 phase. The decomposition enthalpies into PbH$_4$ + 2H$_2$, PbH$_3$ + 5/2H$_2$, PbH$_2$ + 3H$_2$, PbH + 7/2H$_2$, and Pb + 4H$_2$ were also plotted. The inset exhibits the change of enthalpies induced by ZPE correction, which indicates that the decomposition pressure of the $C2/m$ structure decreases as 133 GPa.

units exist in the high-pressure structures of GeH$_4$ and SnH$_4$. And these H$_2$ units have been found to contribute significantly to the superconductivity. Then, whether can the T_c be improved by intercalating H$_2$ into group-IV hydrides? H$_2$-containing compounds of CH$_4$-H$_2$ have been fabricated up to 30 GPa, such as CH$_4$(H$_2$)$_2$, (CH$_4$)$_2$H$_2$, CH$_4$(H$_2$)$_4$, CH$_4$H$_2$[13]. But both metallization and superconductivity are still lack. For the SiH$_4$-H$_2$ system, the crystal structure, phase diagram, and metallization under pressure of SiH$_4$(H$_2$)$_2$ were extensively explored[14–22]. The T_c of SiH$_4$(H$_2$)$_2$ is as high as 107 K at 250 GPa[23], which is visibly higher than that of SiH$_4$. Following the experimental observation[24], we have also theoretically investigated the structural, phase transition, metallization, and superconductivity of GeH$_4$(H$_2$)$_2$ under pressure[25,26]. The predicted T_c of GeH$_4$(H$_2$)$_2$ is close to 100 K at 250 GPa, higher than that of GeH$_4$. These results inevitably encourage us further to seek for high-temperature superconductors and study the superconductivity in these H$_2$-containing compounds. However, it is necessary to decrease the work pressure of superconducting. For examples, the decomposition pressures are as high as 248 GPa for SiH$_4$(H$_2$)$_2$ and 220 GPa for GeH$_4$(H$_2$)$_2$, respectively, above which they are stable superconducting materials.

As mentioned above, the combination the lightest H with one of the heaviest Pb seems to be a good way to improve the T_c and decrease the work pressure. Chemically, PbH$_4$ still remains the most elusive of group-IV tetrahydrides. The pioneering theoretical work of Desclaux and Pyykkö predicted the structure and stability of PbH$_4$[27,28]. The theoretically predicted tetrahedral structure of an isolated molecule, with an equilibrium Pb-H distance of approximately 1.73 Å, was eventually confirmed by experiments[29,30]. But, Krivtsun *et al.*[30] observed that the PbH$_4$ molecules were kinetically unstable and readily decompose to Pb atomic layer and H$_2$ in approximately 10 s. Recently, Zaleski-Ejgierd *et al.* theoretically investigated the structure and the stability of PbH$_4$ under high pressure[31]. They found that PbH$_4$ is stable thermodynamically above 132 GPa, in forms of *Imma* (132–296 GPa) and *Ibam* (>296 GPa) space groups. And PbH$_4$ even keeps the metallic character covering the whole range of pressure[31]. However, the superconductivity is indeterminate, since the dynamic stable phase of PbH$_4$ has been not discovered from experimental and theoretical aspects yet. By intercalating H$_2$ units into PbH$_4$ molecular crystal, e.g. PbH$_4$(H$_2$)$_2$, how about the structure, stability, and superconductivity? It is just the purpose of our study. In this work, we found out the stable phase of PbH$_4$(H$_2$)$_2$ thermodynamically and dynamically and investigated its desired superconductivity. The decomposition pressure of 133 GPa is much lower than the metallization pressure of solid hydrogen, which is easily reached in experiments by diamond-anvil techniques. And the H$_2$-H$_2$ coupling under high pressure figures out the different superconducting mechanism.

Results
Covering the wide pressure range of 0–400 GPa, variable-cell structure prediction simulations with 1 to 4 PbH$_4$(H$_2$)$_2$ formula units per cell (f.u./cell) were performed. We have calculated the enthalpies of searched structures of PbH$_4$(H$_2$)$_2$ to examine the thermodynamical stability induced by pressure. For several competitive structures of PbH$_4$(H$_2$)$_2$, the enthalpies (relative to the P-1 structure) as function of pressure are shown in Fig. 1. It is found that *Pnnm* phase is the most stablest below 40 GPa with the lowest enthalpy value. Starting from 40 GPa up to 135 GPa, PbH$_4$(H$_2$)$_2$ transfers into P-1 phase. Upon further compression, the $C2/m$ becomes to the most stablest phase above 135 GPa. As a result, there are two structural phase transitions existing in the range of 0–400 GPa. Three low-enthalpy structures were obtained, orthorhombic *Pnnm* (4 f.u./cell), triclinic P-1 (2 f.u./cell), and monoclinic $C2/m$ (2 f.u./cell), respectively, as shown in Supplementary Fig. S1 online. The lattice parameters of these three structures at
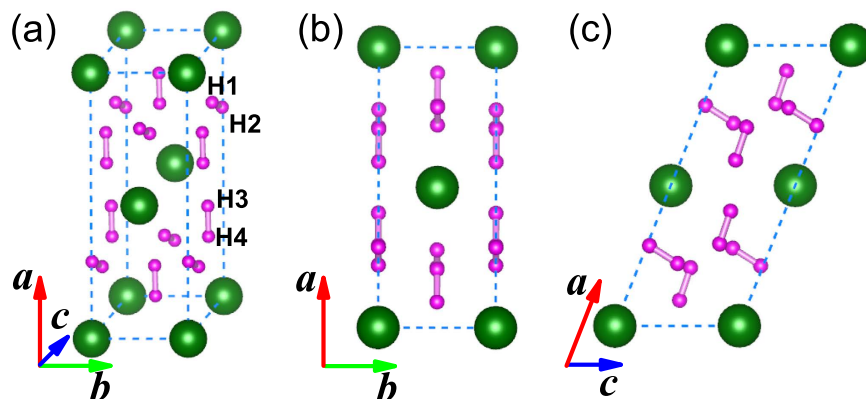
Figure 2. High-pressure crystal structure of $PbH_4(H_2)_2$. (a) $C2/m$ structure at 200 GPa. Large and small spheres represent Pb and H atoms, respectively. H1-H4 mark four non-equivalent H atoms on the crystallographic sites. **(b,c)** show the $C2/m$ structure normal to the (001) and (010) plane, respectively.

different pressures are also listed in Table S1 of the supplementary information online. From the crystal configurations at different pressures, PbH_4 tetrahedral molecule does not exist in $PbH_4(H_2)_2$, and all of hydrogen atoms construct the H_2 quasi-molecules separating from Pb atoms.

However, it was reported that the hydrogen-rich materials is easily decomposed[10,11,15–17,22–25,31,32]. Hence, we must check the stability by mean of estimating the decomposition enthalpy. For $PbH_4(H_2)_2$, there are five possible decomposition paths as $PbH_4(H_2)_2 \rightarrow Pb + 4H_2$, $2PbH_4(H_2)_2 \rightarrow 2PbH + 7H_2$, $PbH_4(H_2)_2 \rightarrow PbH_2 + 3H_2$, $2PbH_4(H_2)_2 \rightarrow 2PbH_3 + 5H_2$, and $PbH_4(H_2)_2 \rightarrow PbH_4 + 2H_2$, respectively. For three system of PbH_3, PbH_2, and PbH, we searched their structures at different pressures. Structural parameters at different pressure regions are presented in Supplementary (Tables S2, S3, and S4) online. With help of the reported structures of $Pmnm$, $P6/mmm$, $Imma$ and $Ibam$ for PbH_4[31], fcc, hcp and $Im\bar{3}m$ for Pb[33], $P6_3m$, $C/2c$, and $Cmca$ for H_2[34] corresponding stable pressures, the decomposition enthalpies were calculated and plotted in Fig. 1. $PbH_4(H_2)_2$ is unstable and decomposes into $Pb + 4H_2$ blow 120 GPa and $PbH_4 + 2H_2$ in the pressure range of 120–160 GPa. Namely, both $Pnnm$ and P-1 phases are metastable. $PbH_4(H_2)_2$ is only stabilized above the pressure of 160 GPa, displaying the symmetry of $C2/m$.

Besides, it has well-known that quantum effects related to hydrogen atoms are very important. The hydrogen zero-point energy (ZPE) has significantly revised the structural stability as in the cases of solid hydrogen[34] and hydrogen-rich materials[9,11]. To judge the effect on stability, we also calculated the ZPEs of $PbH_4(H_2)_2$, PbH_4, and H_2 in the range of 100–200 GPa using the quasiharmonic approximation[35]. As the insert shown in Fig.1, the ZPE effect does not change the order of the phase transitions but lowers the decomposition pressure of the $C2/m$ structure into ~133 GPa. This decomposition pressure of $PbH_4(H_2)_2$ is obviously lower than 248 GPa of $SiH_4(H_2)_2$[23] and 220 GPa of $GeH_4(H_2)_2$[25], which indicates that $PbH_4(H_2)_2$ will exist in the wider pressure range. For this stability, the subsequent crystal structural, electronic, phonon, and electron-phonon coupling (EPC) calculations are focused on the $C2/m$ structure above 133 GPa, and typical results are presented at 200 GPa.

For $C2/m$ structure, Pb atoms occupy the crystallographic $2a$ sites and four non-equivalent H atoms sit on the $4i$ sites under high pressure. All of H atoms pairwise coupling into two types of quasi-molecules as shown in Fig. 2a. The nearest distance between Pb and H atom is about 2 Å. In this dense structure, we can not find any plumbane molecules existing, but H_2 quasi-molecules distribute around Pb atoms and are ordering (Fig. 2). This kind of ordered arrangements of H_2 units is clearer at high pressure, while H_2 units tend to be inordering at low pressure[18,25]. A visible character of Pb and H_2 in layers is observed from (001)-plane (Fig. 2b) or (010)-plane (Fig. 2c). Noticeably, the layered feature is also a common phenomenon in some hydrogen-rich systems. With the increase of pressure, all of the lattice constants of $C2/m$ structure in a, b, and c directions decrease. However, the H-H bond lengths in H_2 quasi-molecules marked as $d1_{H-H}$ (formed by H1 and H2 sites shown in Fig. 2a) and $d2_{H-H}$ (formed by H3 and H4 sites shown in Fig. 2a) firstly increase then decrease as shown in Fig. 3a. There are three kinds of intermolecular distances among H_2 molecules in the $C2/m$ structure, all of them are monotonously decreased with the pressurizing, as shown in Fig. 3b. Reviewing the high-pressure structural character, we find that part hydrogen atoms form H_2 units with the other hydrogen atoms strongly bonding with Si in $Ccca$ phase of $SiH_4(H_2)_2$[23], while all of hydrogen atoms pairwise coupling into H_2 quasi-molecules with the nearest distance of ~1.7 Å between Ge and H in $P2_1/c$ phase of $GeH_4(H_2)_2$[25]. As a comparison, with the help of analysis of atomic distances, the intermolecular and intramolecular couplings of H_2 gradually strengthen, while the interaction between H and the heavy atom evidently weakens from $SiH_4(H_2)_2$ to $GeH_4(H_2)_2$ and then to $PbH_4(H_2)_2$.
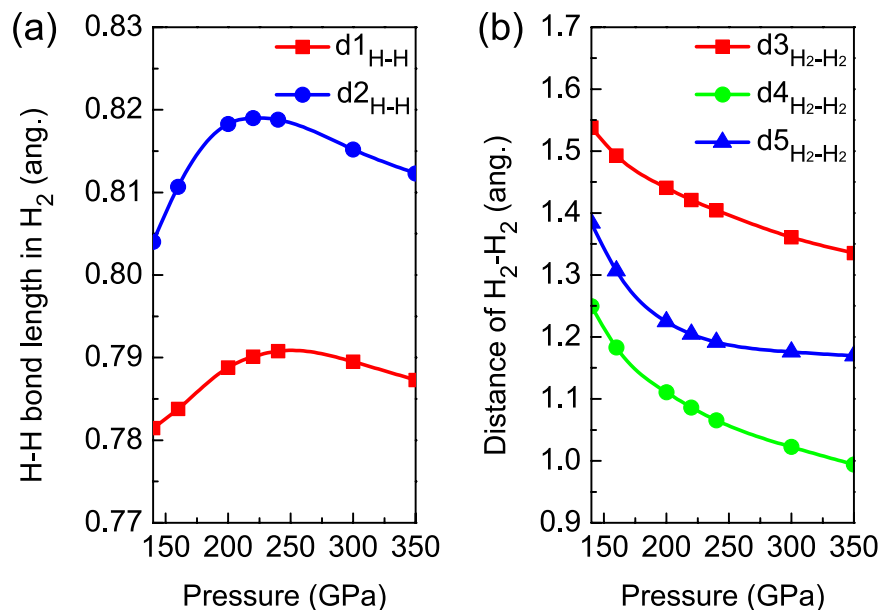
Figure 3. The H-H bond lengths in H$_2$ unit and the H$_2$-H$_2$ intermolecular distances. For *C2/m* structure, two types of H-H bond lengths in H$_2$ (**a**) and three kinds of distances among H$_2$ molecules (**b**) change with pressure (133–350 GPa).

At 200 GPa, the lattice parameters of *C2/m* structure are $a = 7.184$ Å, $b = 2.807$ Å, and $c = 2.973$ Å, as well as the angle $\beta = 68.1°$ (see Supplementary Table S1 online). The d1$_{H-H}$ and d2$_{H-H}$ are 0.78 Å and 0.82 Å, respectively. The intermolecular distance of H$_2$-H$_2$ is less than that between Pb and H atoms. With the lattice parameters, calculated electronic structures show that PbH$_4$(H$_2$)$_2$ is metallic at 200 GPa. For SiH$_4$(H$_2$)$_2$ and GeH$_4$(H$_2$)$_2$ reported previously, they remain the characteristics of insulator under low pressure. The insulator-to-metal transition occurs at 92 GPa in SiH$_4$(H$_2$)$_2$ and at 48 GPa in GeH$_4$(H$_2$)$_2$, respectively. However, we didn't find the transition point of PbH$_4$(H$_2$)$_2$. It seems to be metal even in ambient pressure, which consist with PbH$_4$[31]. So the low pressure metallization does not come from the intercalation of H$_2$ molecules. Comparing with Si and Ge, Pb has larger ionic radius which results in more strong itinerant property of valent electrons. Figure 4 shows the projected density of state (PDOS) at several selected pressures. According to the electronic PDOS at Fermi level we can draw a conclusion that at low pressure in *Pnnm* structure the Pb-*p* electrons make the most contribution to density of state and exhibit properties of a nearly free-electron metal (Fig. 4a,b). As the pressure increases, the strengthening of H$_2$-H$_2$ interaction leads to the overlap of H-*s* wave functions. The contribution of H-*s* electrons to Fermi surface increases. PDOS tends to be uniform distribution, and the bandwidth further broadens from 100 GPa to 300 GPa (Fig. 4c–f). It indicates that with the increase of pressure PbH$_4$(H$_2$)$_2$ mainly like to be Pb-H$_2$ alloy. The Pb interlayer interaction is connected by these H$_2$ molecules. To gain more insight into the bonding nature of PbH$_4$(H$_2$)$_2$, the electron location function (ELF) of *C2/m* phase at 200 GPa was calculated. ELF shown in Fig. 5 displays the electronic location around Pb and H atoms as well as the nearly free-electron-like distribution among Pb atoms. However, the high ELF values between Pb and H atoms (Fig. 5a) and of intermolecular H$_2$ (Fig. 5b) indicate that the electrons become delocalized, suggesting a feature of nearly free-electron metal.

The phonon dispersion curves for *C2/m* structure at 200 GPa (Fig. 6) and other selected pressure point (see Supplementary Fig. S2 online) were calculated to explore the lattice dynamics of PbH$_4$(H$_2$)$_2$. The absence of any imaginary frequencies implies the dynamical stability of *C2/m* phase under high pressure. The whole phonon spectrum can be divided into three parts. By combining with the phonon density of states (PhDOS) projected on atoms shown in Fig. 7a, in the case of 200 GPa, we find that the low-frequency vibration below 215 cm^{-1} mainly come from the vibrations Pb atoms. The intermolecular strong phonon coupling among H$_2$ molecules appear in the intermediate-frequency range of 295–1876 cm^{-1}. After a large gap, in high frequency area above 2695 cm^{-1}, the H-H vibration in H$_2$ formed by H3 and H4 sites mainly contributes in the range of 2695–2898 cm^{-1}, while the vibration in H$_2$ formed by H1 and H2 sites around 3220 to 3380 cm^{-1}. Comparing these three systems of Si-, Ge-, and Pb-based, we find a strong phonon coupling between silicon and hydrogen in SiH$_4$(H$_2$)$_2$[23], very weak phonon coupling between metal and hydrogen in GeH$_4$(H$_2$)$_2$[25] as well as PbH$_4$(H$_2$)$_2$. The H-H vibration in H$_2$ molecule is the strongest in PbH$_4$(H$_2$)$_2$. From the Eliashberg phonon spectral function $\alpha^2F(\omega)$ and the integrated EPC parameter $\lambda(\omega)$ shown in Fig. 7b, the intermediate-frequency (295–1876 cm^{-1}) vibrational modes of H$_2$ molecules contribute 81.5% of total λ. This percentage is larger than 66% in
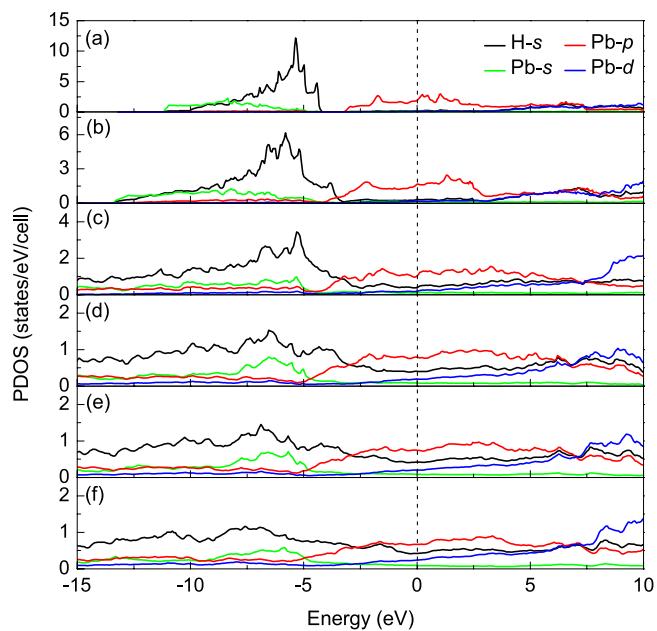
Figure 4. Electronic PDOS at different pressures. Calculated PDOS of $PbH_4(H_2)_2$ at different pressures of 5 GPa (**a**) and 20 GPa (**b**) for P-1 phase, 100 GPa for $Pnnm$ phase (**c**), 160 GPa (**d**), 200 GPa (**e**), and 300 GPa (**f**) for $C2/m$ phase. The lines at zero indicate the Fermi level.

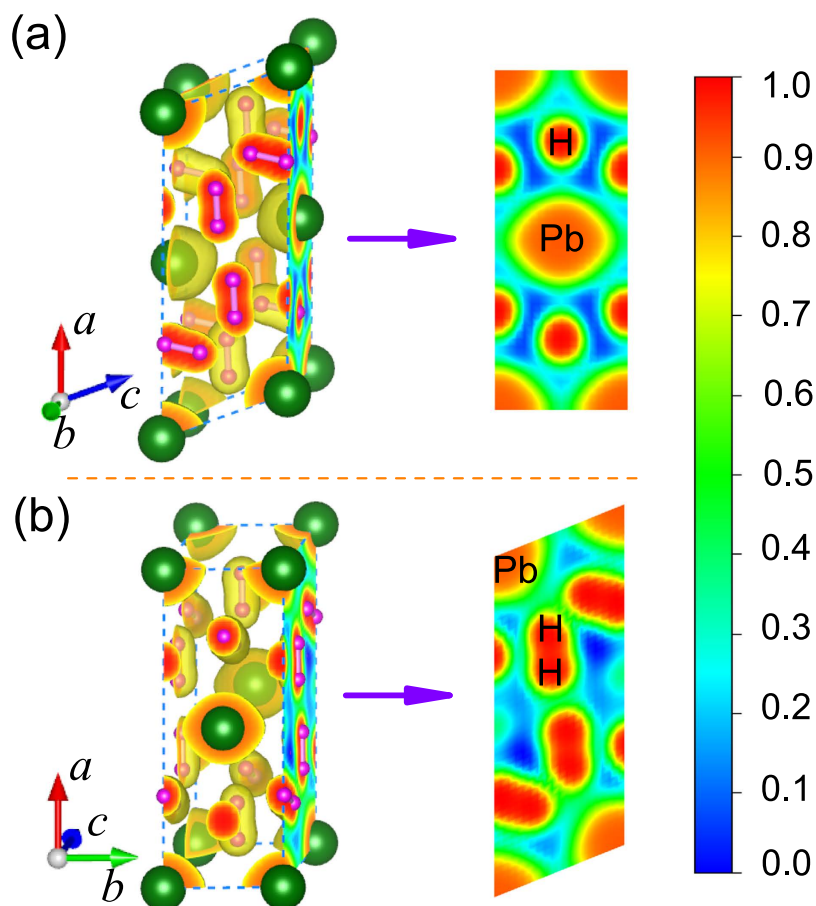**Figure 5. ELF of $PbH_4(H_2)_2$.** Calculated ELF isosurface of $PbH_4(H_2)_2$ for $C2/m$ at 200 GPa with the ELF value of 0.75. (**a,b**) highlight the sections on (001) and (010) planes, respectively.
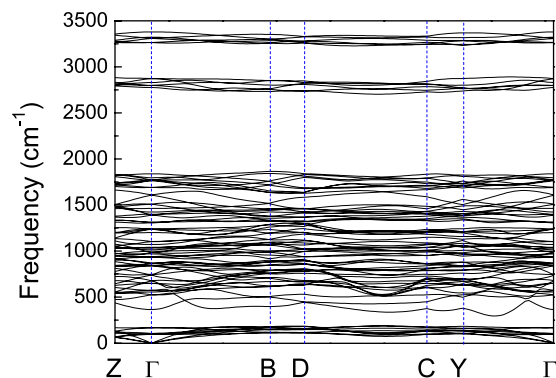
Figure 6. Phonon spectrum. Calculated phonon spectrum of $C2/m$ structure at 200 GPa.
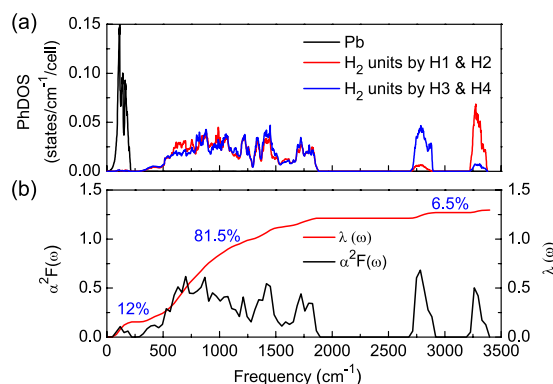

Figure 7. Phonon properties and Eliashberg spectral function. Calculated phonon density of states (PhDOS) (**a**), and the Eliashberg phonon spectral function $\alpha^2F(\omega)$ and electron-phonon integral $\lambda(\omega)$ (**b**) for the $C2/m$ structure at 200 GPa.

Si-based and 75% in Ge-based case. This result highlights the significant role played by H_2 molecules on the electron-phonon interaction.

At 200 GPa, the calculated total EPC constant λ is 1.296 for $C2/m$ $PbH_4(H_2)_2$. From Si to Ge and then to Pb case, the λ gradually decreases from 1.625 to 1.43 and then to 1.296, which implies a weak coupling between metal and hydrogen. However, the phonon frequency logarithmic average ω_{log} rises gradually, from 871 K in $SiH_4(H_2)_2$ to 1051 K in $PbH_4(H_2)_2$. This means more higher Debye temperature in $PbH_4(H_2)_2$. Based on the obtained $\alpha^2F(\omega)$ and $\lambda(\omega)$, we now can analyze the superconductivity using the modified McMillan equation by Allen and Dynes[36],

$$T_c = \frac{\omega_{log}}{1.2} exp\left(-\frac{1.04(1+\lambda)}{\lambda - \mu^*(1+0.62\lambda)}\right). \tag{1}$$

With the typical choice of the Coulomb pseudopotential $\mu^* = 0.1^3$, a remarkable large T_c of 103 K was obtained for $C2/m$ phase of $PbH_4(H_2)_2$, which is comparable with those of copper oxide superconductors.

To figure out the pressure effect on superconductivity in $PbH_4(H_2)_2$, in addition, the T_c values at several typical pressure points were calculated and shown in Supplementary Fig. S3 online. An interesting phenomenon exhibits the superconductivity firstly strengthening before weakening. The T_c has a maximum between 140 and 350 GPa, ~107 K for $\mu^* = 0.1$. Seen from the distances of among H_2 molecules shown in Fig. 3b, the monotonously decreasing makes a hint of "hardening" of intermediate-frequency phonon with the increase of pressure. The phonon spectra shown in Supplementary Fig. S2 online confirm this point. To analyze this phenomenon of T_c variations, we have further calculated the Eliashberg phonon spectral function and the EPC strength at different pressures, the results are presented in Supplementary Fig. S4 online. With the increase of pressure, the calculated EPCs are 1.280, 1.296, 1.379, and 1.341 for 180 GPa, 200 GPa, 250 GPa, and 300 GPa, respectively, which shows a tendency of first increase and then decrease similar to T_c. In the T_c rising zone, the contribution of Pb-H coupling to the EPC strength is decreased from 14.3% at 180 GPa to 12% at 200 GPa, and the phonon vibration of H-H

in H_2 units also weakens the EPC (The contribution is from 7.3% to 6.5% corresponding pressures.). However, the contribution of H_2-H_2 coupling to the EPC is strengthening from 78.4% at 180 GPa to 81.5% at 200 GPa. So the initial rising of T_c results from the contribution increasing of H_2-H_2 for the EPC. As shown in Fig. S4 online, from 75.8% at 250 GPa to 73.5% at 300 GPa, the decrease of contribution of H_2-H_2 for the EPC leads to the fall of T_c. The result further reveals the significance of H_2-H_2 coupling to superconductivity in $PbH_4(H_2)_2$.

Discussion

Thus far, the stability of $PbH_4(H_2)_2$ has been identified in the pressure range of 0–400 GPa. At low pressure it is metastable and possibly decomposes into $Pb + H_2$ or $PbH_4 + H_2$. Above 133 GPa, it is stable not only thermodynamically but also dynamically. This high-pressure stable phase of $C2/m$ exhibits the expected superconductivity of $T_c \sim 107$ K at 230 GPa, which is obviously higher than those of conventional group-IV hydrides such as silane, germane, and stannane. Noticeably, the coupling between group-IV element and hydrogen reduces with the increase of atomic number. Namely, the contribution of group-IV element to total EPC decreases in hydrides from 33% in $SiH_4(H_2)_2$[23] to 25% in $GeH_4(H_2)_2$[25] and then to 12% in $PbH_4(H_2)_2$. On the contrary, the coupling among H_2 molecules strengthens as mentioned above. Particularly, we want to point out that the T_c (~100 K) is comparable for $SiH_4(H_2)_2$, $GeH_4(H_2)_2$, and $PbH_4(H_2)_2$ at the same Coulomb pseudopotential, though the superconducting mechanism is incompletely same. The intercalating H_2 molecules into group-IV hydrides really improves the T_c. From the phonon contribution to EPC, we find that the intermediate-frequency phonon is dominated. Comparing with corresponding SiH_4[8], GeH_4[11], and SnH_4[12], it is clear that the intercalation of H_2 molecules results in the softening of intermediate-frequency phonon. As increasing the content of hydrogen in group-IV elements, it results in enhancing the EPC strength that is dominated by the coupling of the H_2 molecular in the $AH_4(H_2)_2$ (A = Si, Ge, Sn, and Pb) crystals. This is just the origin of higher T_c in H_2-containing compounds. Furthermore, we infer that the higher T_c may be obtained if more H_2 are inserted in group-IV hydrides. Actually, more future works are needed to advance the T_c and understand the superconductivity.

As a comparison, the high-pressure structure of $PbH_4(H_2)_2$ is visibly different from other hydrogen-rich compounds with high T_c, such as CaH_6[37] and $(H_2S)_2H_2$[32]. In high-pressure structures of CaH_6 and $(H_2S)_2H_2$, the H_2 quasi-molecules have been broken, with the strong bonds forming between metal and hydrogen atoms. Although the EPC is mainly contributed by hydrogen, the superconducting mechanism is different. It is the H-H coupling in CaH_6 and $(H_2S)_2H_2$, while the H_2-H_2 coupling in $PbH_4(H_2)_2$. It is interested that the H_2 quasi-molecule form keeps all along at thus high pressure up to 400 GPa. At the same time, Pb is one of the heaviest elements. The combination with the lightest H is one of the most important physical problems in high-pressure research. Pb metal makes the metallization pressure of hydrogen-rich compound decrease. Remarkably, the decomposition pressure point (133 GPa) of $PbH_4(H_2)_2$ is the lowest among these H_2-containing compounds of Si-, Ge-, and Pb-based. This value is much lower than the metallization pressure of bulk molecular hydrogen, which indicates the feasibility to experimentally observe. Hence, Pb-based hydrides are the potential candidates as high-T_c superconductors. Our finding may hopefully stimulate the potential high-T_c superconductors research in H_2-containing hydrides.

Methods

The search for crystalline structures of $PbH_4(H_2)_2$ phases was performed using particle swarm optimization methodology as implemented in the CALYPSO program[38,39]. Structural optimizations, enthalpies, and electronic structures were calculated using the Vienna ab initio simulation (VASP) program[40,41] and projector-augmented plane wave (PAW) potentials employing the Perdew-Burke-Ernzerhof (PBE) functional[42]. The $1s^1$ and $6s^26p^2$ electrons were included in the valence space for H and Pb atoms, respectively. For the plane-wave basis-set expansion, an energy cutoff of 800 eV was used. Dense k-point meshes were employed to sample the first Brillouin zone (BZ) and ensured that energies converged to within 1 meV/atom. All forces acting on atoms were converged 0.001 eV/Å or less, and the total stress tensor was reduced to the order of 0.01 GPa. With the noteworthy mass ratio 207:1 between Pb and H, we have involved the spin-orbit effect in this calculation.

Based on the optimized structures from VASP, lattice dynamics and superconducting properties were calculated using density functional perturbation theory[43] and the Troullier-Martins norm-conserving potentials[44], as implemented in the QUANTUMESPRESSO code[45]. The cutoff energies of 60 and 400 Ry were used for wave functions and charge densities, respectively. $12 \times 12 \times 8$ Monkhorst-Pack k-point grid with Gaussian smearing of 0.03 Ry was used for the phonon calculations at $3 \times 3 \times 2$ q-point mesh, and double k-point grid was used in the calculation of the electron-phonon interaction matrix element.

References

1. Ashcroft, N. W. Metallic Hydrogen: A High-Temperature Superconductor? *Phys. Rev. Lett.* **21,** 1748 (1968).
2. Narayana, C., Luo, H., Orloff, J. & Ruoff, A. L. Solid hydrogen at 342 GPa: no evidence for an alkali metal. *Nature* **393,** 46–49 (1998).
3. Ashcroft, N. W. Hydrogen Dominant Metallic Alloys: High Temperature Superconductors? *Phys. Rev. Lett.* **92,** 187002 (2004).
4. Martinez-Canales, M. & Bergara, A. No evidence of metallic methane at high pressure. *High Pressure Res.* **26,** 369–375 (2006).

5. Eremets, M. I., Trojan, I. A., Medvedev, S. A., Tse, J. S. & Yao, Y. Superconductivity in Hydrogen Dominant Materials: Silane. *Science* **319,** 1506–1509 (2008).
6. Zhou, X. F. *et al.* Superconducting high-pressure phase of platinum hydride from first principles. *Phys. Rev. B* **84,** 054543 (2011).
7. Kim, D. Y., Scheicher, R. H., Pickard, C. J., Needs, R. J. & Ahuja, R. Predicted Formation of Superconducting Platinum-Hydride Crystals under Pressure in the Presence of Molecular Hydrogen. *Phys. Rev. Lett.* **107,** 117002 (2011).
8. Martinez-Canales, M. *et al.* Novel Structures and Superconductivity of Silane under Pressure. *Phys. Rev. Lett.* **102,** 087005 (2009).
9. Zhang, C. *et al.* Superconductivity in Hydrogen-rich Material: GeH_4. *J. Supercond. Nov. Magn.* **23,** 717–719 (2010).
10. Zhang, C. *et al.* Structural transitions of solid germane under pressure. *Europhys. Lett.* **90,** 66006 (2010).
11. Gao, G. *et al.* Superconducting High Pressure Phase of Germane. *Phys. Rev. Lett.* **101,** 107002 (2008).
12. Tse, J. S., Yao, Y. & Tanaka, K. Novel Superconductivity in Metallic SnH_4 under High Pressure. *Phys. Rev. Lett.* **98,** 117004 (2007).
13. Somayazulu, M. S., Finger, L. W., Hemley, R. J. & Mao, H. K. High-Pressure Compounds in Methane-Hydrogen Mixtures. *Science* **271,** 1400–1402 (1996).
14. Wang, S., Mao, H. K., Chen, X. J. & Mao, W. L. High pressure chemistry in the H_2-SiH_4 system. *Proc. Natl. Acad. Sci. USA* **106,** 14763–14767 (2009).
15. Strobel, T. A., Somayazulu, M. & Hemley, R. J. Novel Pressure-Induced Interactions in Silane-Hydrogen. *Phys. Rev. Lett.* **103,** 065701 (2009).
16. Yao, Y. & Klug, D. D. Silane plus molecular hydrogen as a possible pathway to metallic hydrogen. *Proc. Natl. Acad. Sci. USA* **107,** 20893–20898 (2010).
17. Yim, W. L., Tse, J. S. & Iitaka, T. Pressure-Induced Intermolecular Interactions in Crystalline Silane-Hydrogen. *Phys. Rev. Lett.* **105,** 215501 (2010).
18. Li, Y., Gao, G., Li, Q., Ma, Y. & Zou, G. Orientationally disordered H_2 in the high-pressure van der Waals compound $SiH_4(H_2)_2$. *Phys. Rev. B* **82,** 064104 (2010).
19. Chen, X. Q., Wang, S., Mao, W. L. & Fu, C. L. Pressure-induced behavior of the hydrogen-dominant compound $SiH_4(H_2)_2$ from first-principles calculations. *Phys. Rev. B* **82,** 104115 (2010).
20. Michel, K., Liu, Y. & Ozolins, V. Atomic structure and SiH_4-H_2 interactions of $SiH_4(H_2)_2$ from first principles. *Phys. Rev. B* **82,** 174103 (2010).
21. Shanavas, K. V., Poswal, H. K. & Sharma, S. M. First principles calculations on the effect of pressure on $SiH_4(H_2)_2$. *Solid State Commun.* **152,** 873–877 (2012).
22. Wei, Y. K. *et al.* Pressure induced metallization of $SiH_4(H_2)_2$ via first-principles calculations. *Comp. Mater. Sci.* **88,** 116–123 (2014).
23. Li, Y. *et al.* Superconductivity at ~100 K in dense $SiH_4(H_2)_2$ predicted by first principles. *Proc. Natl. Acad. Sci. USA* **107,** 15708–15711 (2010).
24. Strobel, T. A., Chen, X. J., Somayazulu, M. & Hemley, R. J. Vibrational dynamics, intermolecular interactions, and compound formation in GeH_4-H_2 under pressure. *J. Chem. Phys.* **133,** 164512 (2010).
25. Zhong, G. *et al.* Structural, Electronic, Dynamical, and Superconducting Properties in Dense $GeH_4(H_2)_2$. *J. Phys. Chem. C* **116,** 5225–5234 (2012).
26. Zhong, G. *et al.* Superconductivity in $GeH_4(H_2)_2$ above 220 GPa high-pressure. *Physica B* **410,** 90–92 (2013).
27. Desclaux, J. P. & Pyykkö, P. Relativistic and non-relativistic Hartree-Fock one-centre expansion calculations for the series CH_4 to PbH_4 within the spherical approximation. *Chem. Phys. Lett.* **29,** 534 (1974).
28. Pyykkö, P. & Desclaux, J. P. Dirac-Fock one-centre calculations show $(114)H_4$ to resemble PbH_4. *Nature* **266,** 336–337 (1977).
29. Wang, X. & Andrews, L. Infrared spectra of group 14 hydrides in solid hydrogen: experimental observation of PbH_4, Pb_2H_2, and Pb_2H_4. *J. Am. Chem. Soc.* **125,** 6581–6587 (2003).
30. Krivtsun, V. M., Kuritsyn, Y. A. & Snegirev, E. P. Observation of IR absorption spectra of the unstable PbH_4 molecule. *Opt. Spectrosc.* **86,** 686–691 (1999).
31. Zaleski-Ejgierd, P., Hoffmann, R. & Ashcroft, N. W. High Pressure Stabilization and Emergent Forms of PbH_4. *Phys. Rev. Lett.* **107,** 037002 (2011).
32. Duan, D. *et al.* Pressure-induced metallization of dense $(H_2S)_2H_2$ with high-T_c superconductivity. *Sci. Rep.* **4,** 6968 (2014).
33. Liu, A. Y., Garca, A., Cohen, M. L., Godwal, B. K. & Jeanloz, R. Theory of high-pressure phases of Pb. *Phys. Rev. B* **43,** 1795 (1991).
34. Pickard, C. J. & Needs, R. J. Structure of phase III of solid hydrogen. *Nat. Phys.* **3,** 473–476 (2007).
35. Ma, Y. & Tse, J. S. Ab initio determination of crystal lattice constants and thermal expansion for germanium isotopes. *Solid State Commun.* **143,** 161–165 (2007).
36. Allen, P. B. & Dynes, R. C Transition temperature of strong-coupled superconductors reanalyzed. *Phys. Rev. B* **12,** 905 (1975).
37. Wang, H., Tse, J. S., Tanaka, K., Iitaka, T. & Ma, Y. Superconductive sodalite-like clathrate calcium hydride at high pressures. *Proc. Natl. Acad. Sci. USA* **109,** 6463–6466 (2012).
38. Wang, Y., Lv, J., Zhu, L. & Ma, Y. Crystal structure prediction via particle-swarm optimization. *Phys. Rev. B* **82,** 094116 (2010).
39. Wang, Y., Lv, J., Zhu, L. & Ma, Y. CALYPSO: A Method for Crystal Structure Prediction. *Comput. Phys. Commun.* 183, 2063 (2012).
40. Kresse, G. & Furthmüller, J. Efficiency of ab-initio total energy calculations for metals and semiconductors using a plane-wave basis set. *Comput. Mater. Sci.* **6,** 15–50 (1996).
41. Kresse, G. & Furthmüller, J. Efficient iterative schemes for ab initio total-energy calculations using a plane-wave basis set. *Phys. Rev. B* **54,** 11169 (1996).
42. Perdew, J. P., Burke, K. & Ernzerhof, M. Generalized Gradient Approximation Made Simple. *Phys. Rev. Lett.* **77,** 3865 (1996).
43. Baroni, S., de Gironcoli, S., Dal Corso, A. & Giannozzi, P. Phonons and related crystal properties from density-functional perturbation theory. *Rev. Mod. Phys.* **73,** 515–562 (2001).
44. Troullier, N. & Martins, J. L. Efficient pseudopotentials for plane-wave calculations. *Phys. Rev. B* **43,** 1993 (1991).
45. Giannozzi, P. *et al.* QUANTUM ESPRESSO: a modular and open-source software project for quantum simulations of materials. *J. Phys.: Condens. Matter* **21,** 395502 (2009).

Acknowledgements

Author Contributions

G.H.Z. and C.L.Y. designed research. Y.C., C.Z. and T.T.W. performed research. Y.C., C.Z., T.T.W., C.L.Y., G.H.Z., X.J.C. and H.Q.L. analyzed the results. Y.C., C.L.Y. and G.H.Z. wrote the first draft of the paper and all authors contributed to revisions. All authors reviewed the manuscript.

Additional Information